Progress In Electromagnetics Research B, Vol. 5, 133–152, 2008

DESIGN OF A TUNABLE POLARIZER USING A ONE-DIMENSIONAL NANO SIZED PHOTONIC BANDGAP STRUCTURE

S. K. Awasthi

Amity Institute of Applied Science
Amity University
Noida-201301, India

U. Malaviya

Department of Physics
University of Lucknow
Lucknow-226007, India

S. P. Ojha

Chaudhary Charan Singh University
Meerut-25004, India

N. K. Mishra and B. Singh

U. P. Autonomous College
Varanasi-221007, India

Abstract—In this paper a transfer matrix treatment for the reflectivity and transmissivity spectra of electromagnetic waves propagating in a nano sized multilayer periodic structure has been presented. Effect of varying the angle of incidence on the photonic bandgaps is shown. The design of a tunable polarizer by reflection which is more efficient in comparison to that obtained by reflection from a single dielectric slab, has been suggested.

1. INTRODUCTION

Photonic crystals (PCs) are artificial multi-dimensional periodic structures with a period of the order of optical wavelength, which can prohibit the propagation of light in specific wavelength ranges [1]. These ranges called the photonic bandgaps are angle dependent, due to the differing periodicities experienced by light propagating at non-normal incidences [2]. Electromagnetic propagation in periodic media has been studied extensively [3–5]. Photonic crystals have found application in lasers [6–8], fibers [9], splitters [10], and many other fields [11]. PCs have drawn much attention as a new kind of optical materials [12, 13]. These materials have many potential applications in optoelectronics and optical communication [13–26].

Polarizers and polarizing beam splitters (PBSs) have found application in many optical systems. Whereas in a polarizer it is only the transmitted or the reflected light that is utilized, in a polarizing beam splitter both the transmitted and the reflected beams are utilized and are of equal significance [27]. A photonic crystal polarizer based on the Brewster angle effect is far more efficient than the well known pile of plates polarizer at Brewster's angle [28], firstly, because absorption losses are almost negligible in PCs, and secondly, because the general Brewster stack works only at Brewster's angle, whereas the photonic crystal polarizer, by proper designing, can be made to operate quite efficiently over a wide angular range of the incident light.

In this paper a transfer matrix method (TMM) [29, 30] to study the reflectivity and transmissivity spectra for light waves impinging on a nano sized one-dimensional photonic band gap material has been reported. The effect of varying the angle of incidence on the photonic bandgap is studied. This structure can be used to design a polarizer by reflection which is more efficient than that obtained by reflection at Brewster's angle from a single dielectric slab. The desired wavelength range of maximum efficiency of operation of the polarizer can be achieved by changing the lattice parameters, or the refractive index of the ambient medium, or both. Investigation in the visible range of the electromagnetic spectrum has been carried out.

2. THEORETICAL ANALYSIS

The multilayered structure consists of dielectric slabs stacked periodically along the x axis and placed between semi infinite media of refractive indices n_0 and n_s (Fig. 1). We assume a periodic step

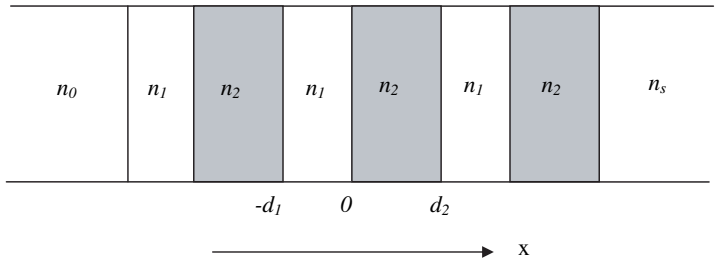

Figure 1. Depiction of a one dimensional periodic lattice.

function for the refractive index of the form [31, 32]

$$n(x) = \begin{cases} n_1, & -d_1 < x < 0, \\ n_2, & 0 < x < d_2, \end{cases} \tag{1}$$

with $n(x) = n(x + md)$ and m is the translational factor which takes values 0, ± 1, ± 2, $---$ and $d = d_1 + d_2$ is the period of the lattice with d_1 and d_2 being the width of the steps having refractive indices n_1 and n_2 respectively.

For the TE wave, the electromagnetic field can be described by a two component wave function [33, 34]

$$\chi = \begin{bmatrix} E_z \\ icB_y \end{bmatrix} \tag{2}$$

where c is the velocity of light in vacuum, E_z and B_y are the tangential components of the electromagnetic field.

The characteristic matrix $M[d]$ of one period is given by [30]

$$M[d] = \prod_{i=1}^{2} \begin{bmatrix} \cos\gamma_i & \frac{-i}{p_i}\sin\gamma_i \\ -ip_i \sin\gamma_i & \cos\gamma_i \end{bmatrix} \equiv \begin{bmatrix} M_{11} & M_{12} \\ M_{21} & M_{22} \end{bmatrix} \tag{3}$$

where $\gamma_i = \frac{2\pi}{\lambda_0} n_i d_i \cos\theta_i$, $p_i = n_i \cos\theta_i$, θ_i is the ray angle inside the layer of refractive index n_i, and is related to the angle of incidence θ_0 of light on the periodic structure by

$$\cos\theta_i = \left[1 - \frac{n_0^2 \sin^2\theta_0}{n_i^2}\right]^{1/2} \tag{4}$$

The matrix $M[d]$ in Equation (3) is unimodular as $|M[d]| = 1$.

For an N period structure, the characteristic matrix of the medium is given by

$$[M(d)]^N = M[Nd] = \begin{bmatrix} m_{11} & m_{12} \\ m_{21} & m_{22} \end{bmatrix} \tag{5}$$

where

$$\begin{aligned} m_{11} &= \left(\cos\gamma_1\cos\gamma_2 - \frac{p_2}{p_1}\sin\gamma_1\sin\gamma_2\right) U_{N-1}(a) - U_{N-2}(a), \\ m_{12} &= -i\left(\frac{1}{p_2}\cos\gamma_1\sin\gamma_2 + \frac{1}{p_1}\sin\gamma_1\cos\gamma_2\right) U_{N-1}(a), \\ m_{21} &= -i(p_1\sin\gamma_1\cos\gamma_2 + p_2\cos\gamma_1\sin\gamma_2) U_{N-1}(a), \\ m_{22} &= \left(\cos\gamma_1\cos\gamma_2 - \frac{p_1}{p_2}\sin\gamma_1\sin\gamma_2\right) U_{N-1}(a) - U_{N-2}(a), \end{aligned}$$

where

$$a = \frac{1}{2}\left[M_{11} + M_{22}\right] = \cos\gamma_1\cos\gamma_2 - \frac{1}{2}\left(\frac{p_1}{p_2} + \frac{p_2}{p_1}\right)\sin\gamma_1\sin\gamma_2, \tag{6}$$

and U_N are the Chebyshev polynomials of the second kind:

$$U_N(a) = \frac{\sin\left[(N+1)\cos^{-1}a\right]}{[1-a^2]^{1/2}} \tag{7}$$

The reflection and transmission coefficients of the multilayer are given by [30]

$$r = \frac{R}{A} = \frac{(m_{11} + m_{12}p_s)p_0 - (m_{21} + m_{22}p_s)}{(m_{11} + m_{12}p_s)p_0 + (m_{21} + m_{22}p_s)} \tag{8}$$

and

$$t = \frac{T}{A} = \frac{2p_0}{(m_{11} + m_{12}p_s)p_0 + (m_{21} + m_{22}p_s)} \tag{9}$$

where

$$p_0 = n_0\cos\theta_0, \quad p_s = n_s\cos\theta_s = n_s\left[1 - \frac{n_0^2\sin^2\theta_0}{n_s^2}\right]^{1/2}$$

where A, R and T are the amplitudes of the electric vectors of the incident, reflected and transmitted waves respectively. Substitution

of expressions [5–7] into [8, 9] will give the reflection and transmission coefficients of the multilayer.

The reflectivity and transmissivity of the multilayer are given by

$$R = |r|^2 = (rr^*), \quad T = \frac{p_s}{p_0}|t|^2 = \frac{p_s}{p_0}(tt^*) \tag{10}$$

The reflectivity and transmissivity of the multilayer for the TM wave can be obtained by using expressions (3)–(10) with the following values of p_i, p_0 and p_s [35]

$$p_i = \frac{\cos\theta_i}{n_i}, \quad (i = 1, 2) \tag{11}$$

$$p_0 = \frac{\cos\theta_0}{n_0}, \quad p_s = \frac{\cos\theta_s}{n_s} = \frac{\left[1 - \dfrac{n_0^2 \sin^2\theta_0}{n_s^2}\right]^{1/2}}{n_s} \tag{12}$$

3. RESULTS AND DISCUSSION

For numerical computation, values of lattice parameters d_1 and d_2 are chosen as $d_1 = 46\,\text{nm}$, $d_2 = 192\,\text{nm}$. A 10-period structure ($N = 10$) has been considered.

Taking $n_0 = n_s = 1.0$ (air), $n_1 = 1.52$ (glass), $n_2 = 1.0$ (air) and using expressions (3)–(10), reflectivity and transmissivity curves for TE and TM waves for varying angles of incidence have been plotted as a function of free space wavelength λ_0 (Fig. 2.1 & Fig. 2.2). These curves indicate that as the incidence angle increases, the photonic bandgap regions, which are the regions of maximum reflectivity, and which coincide with the forbidden band gaps of the periodic structure shift towards the lower wavelength side. Also, the photonic bandgaps for the TE wave are generally wider than the corresponding ones for the TM wave. Figs. 3.1 and 3.2 are a plot of the reflectivity and transmissivity curves for a sharper refractive index contrast i.e., $n_1 = 2.2$ (ZrO_2), $n_2 = 1.0$ (air), $n_0 = n_s = 1.0$ (air). Comparison of Fig. 2 and Fig. 3 shows that a sharper refractive index contrast results in a wider bandgap region for all incidence angles. Table 1.1 shows the photonic bandgap regions for different angles of incidence for the above two cases considered.

4. DESIGN OF A POLARIZER

Figure 2.2(d) indicates that for an incidence angle of 56.70, the reflectivity of the TM wave is zero for the entire visible range

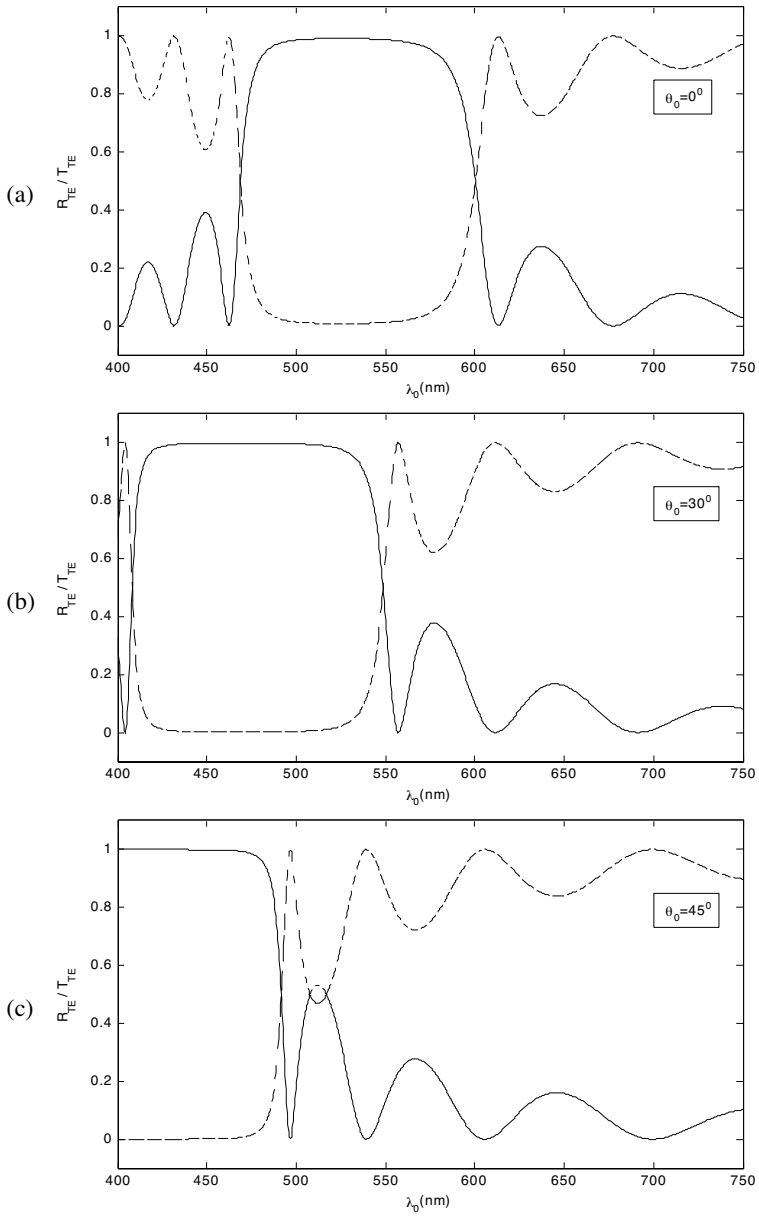

Figure 2.1. Reflectivity (R_{TE}-solid curve) & Transmissivity (T_{TE}-dashed curve) spectra for TE waves at various angles of incidence. ($n_1 = 1.52$, $n_2 = 1.0$, $n_0 = n_s = 1.0$, $d_1 = 46\,\mathrm{nm}$, $d_2 = 192\,\mathrm{nm}$, $N = 10$).

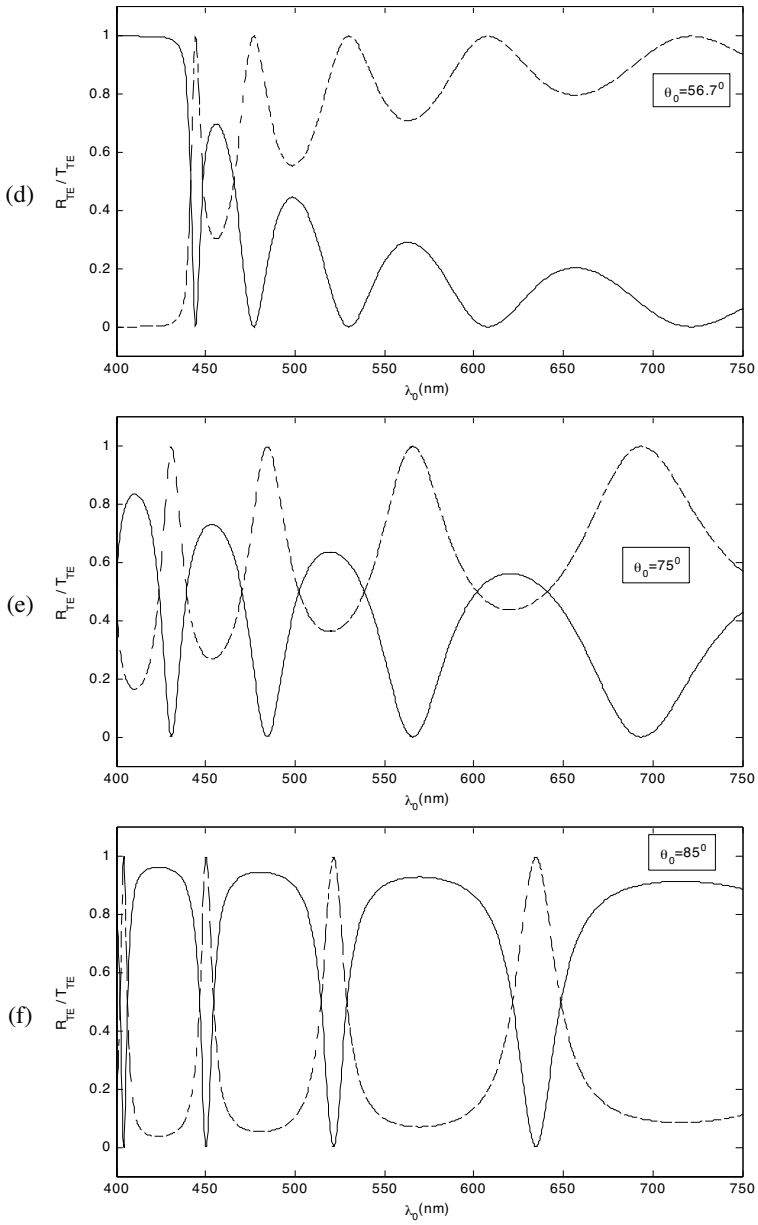

Figure 2.1. Reflectivity (R_{TE}-solid curve) & Transmissivity (T_{TE}-dashed curve) spectra for TE waves at various angles of incidence. ($n_1 = 1.52$, $n_2 = 1.0$, $n_0 = n_s = 1.0$, $d_1 = 46\,\mathrm{nm}$, $d_2 = 192\,\mathrm{nm}$, $N = 10$).

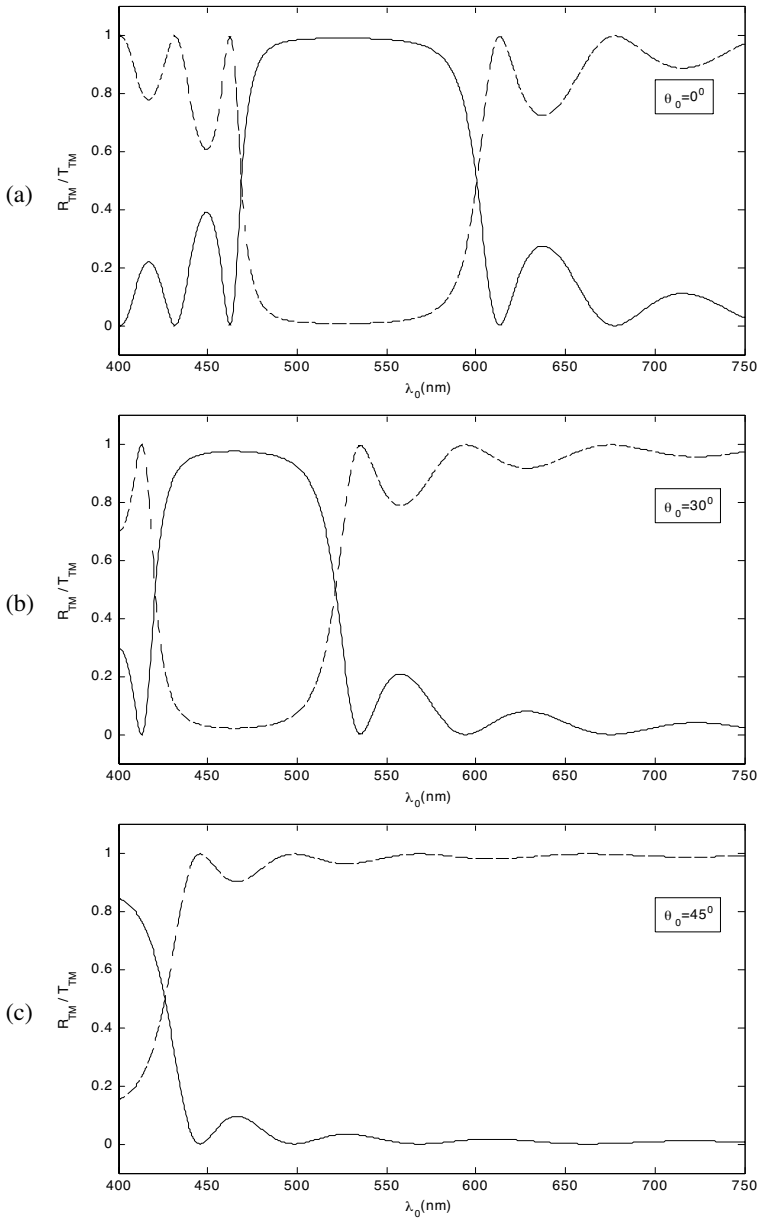

Figure 2.2. Reflectivity (R_{TM}-solid curve) & Transmissivity (T_{TM}-dashed curve) spectra for TM waves at various angles of incidence. ($n_1 = 1.52$, $n_2 = 1.0$, $n_0 = n_s = 1.0$, $d_1 = 46\,\mathrm{nm}$, $d_2 = 192\,\mathrm{nm}$, $N = 10$).

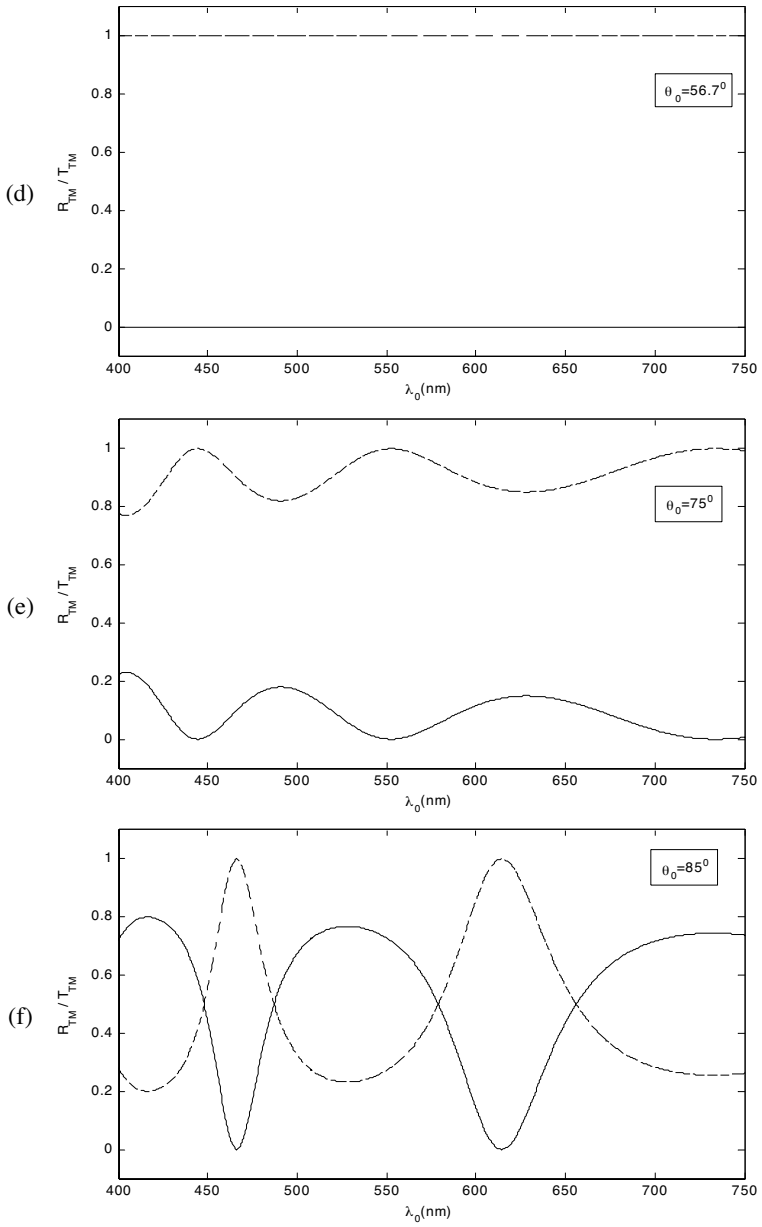

Figure 2.2. Reflectivity (R_{TM}-solid curve) & Transmissivity (T_{TM}-dashed curve) spectra for TM waves at various angles of incidence. ($n_1 = 1.52$, $n_2 = 1.0$, $n_0 = n_s = 1.0$, $d_1 = 46\,\mathrm{nm}$, $d_2 = 192\,\mathrm{nm}$, $N = 10$).

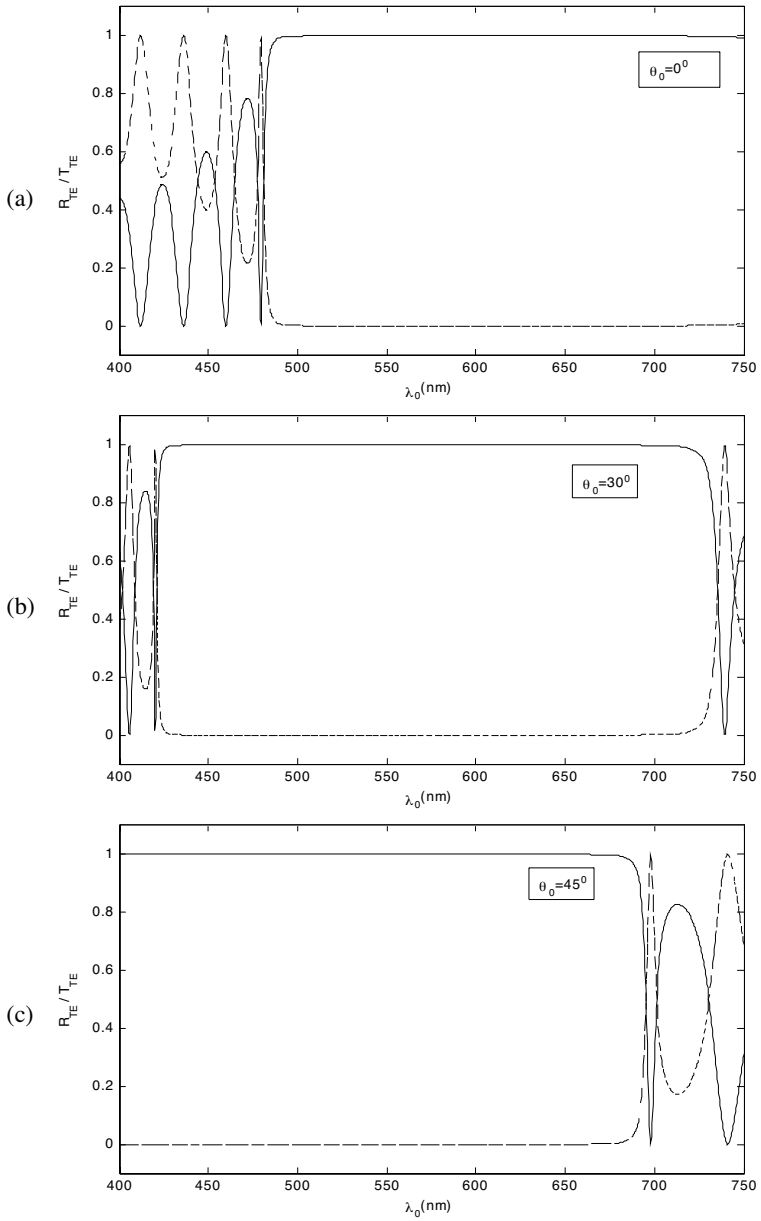

Figure 3.1. Reflectivity (R_{TE}-solid curve) & Transmissivity (T_{TE}-dashed curve) spectra for TE waves at various angles of incidence. ($n_1 = 2.2$, $n_2 = 1.0$, $n_0 = n_s = 1.0$, $d_1 = 46\,\mathrm{nm}$, $d_2 = 192\,\mathrm{nm}$, $N = 10$).

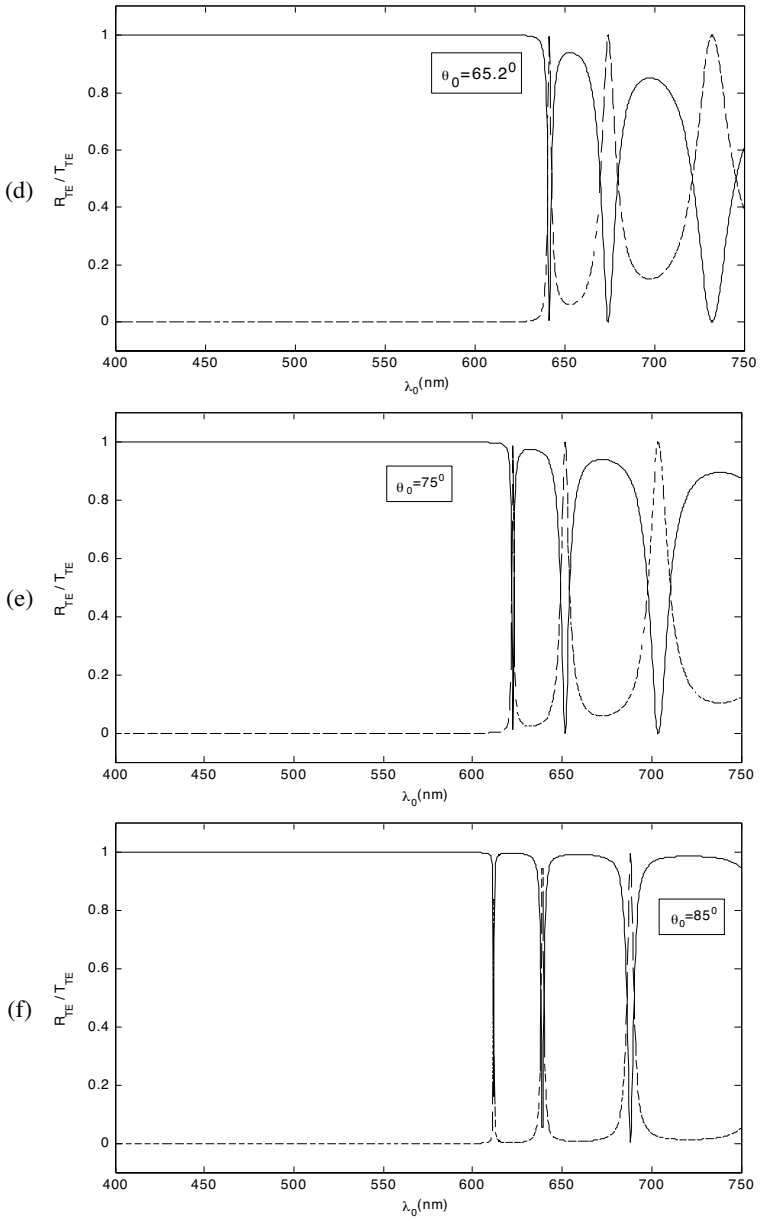

Figure 3.1. Reflectivity (R_{TE}-solid curve) & Transmissivity (T_{TE}-dashed curve) spectra for TE waves at various angles of incidence. ($n_1 = 2.2$, $n_2 = 1.0$, $n_0 = n_s = 1.0$, $d_1 = 46\,\mathrm{nm}$, $d_2 = 192\,\mathrm{nm}$, $N = 10$).

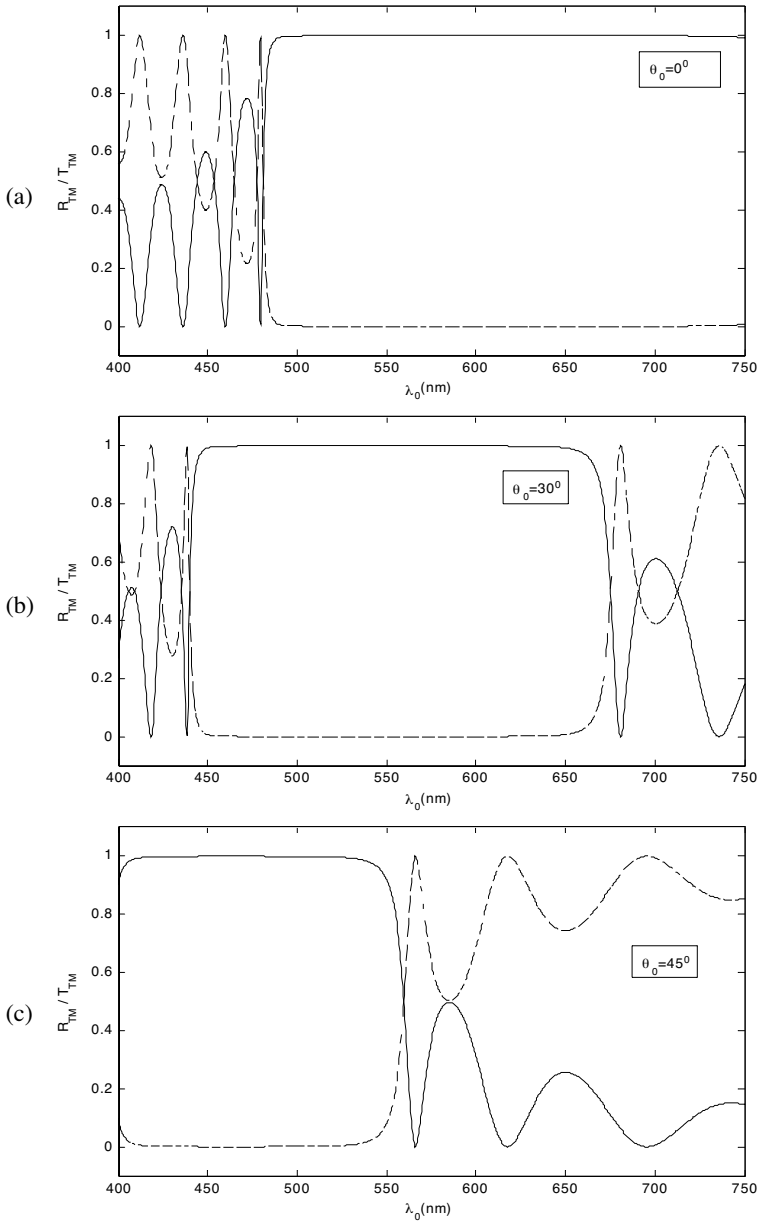

Figure 3.2. Reflectivity (R_{TM}-solid curve) & Transmissivity (T_{TM}-dashed curve) spectra for TM waves at various angles of incidence. ($n_1 = 2.2$, $n_2 = 1.0$, $n_0 = n_s = 1.0$, $d_1 = 46\,\mathrm{nm}$, $d_2 = 192\,\mathrm{nm}$, $N = 10$).

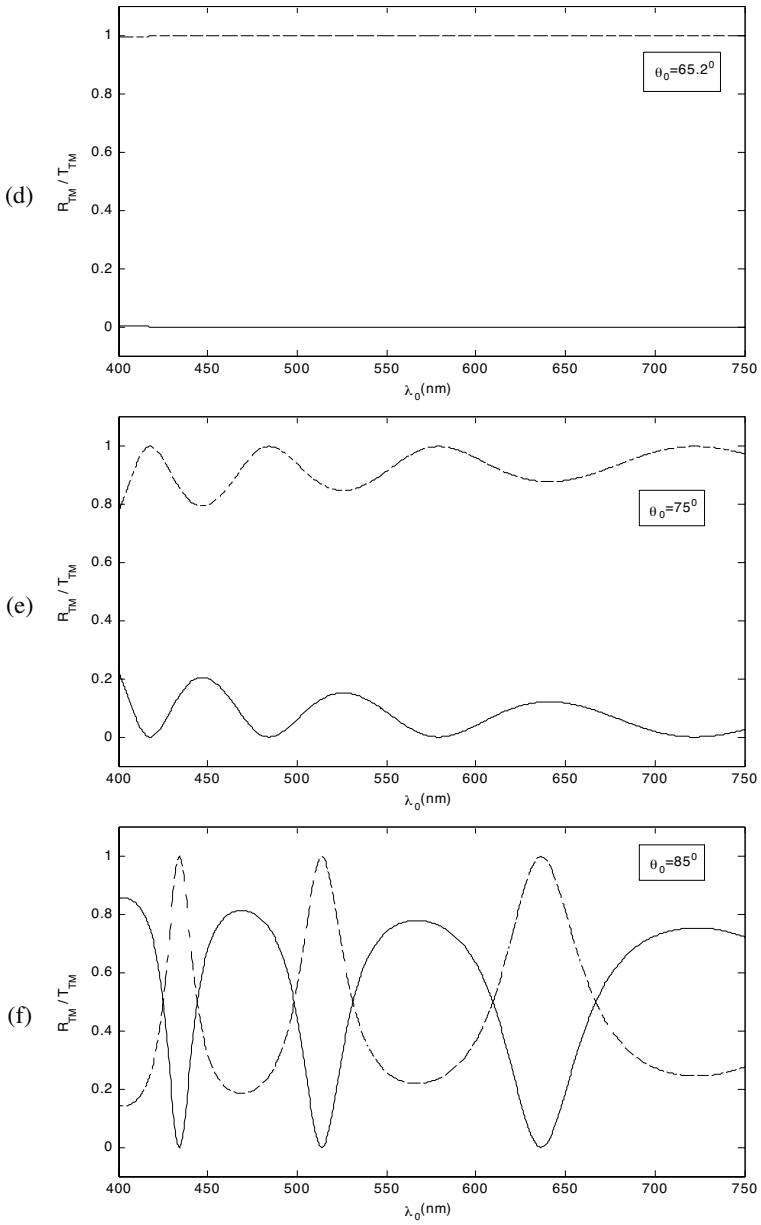

Figure 3.2. Reflectivity (R_{TM}-solid curve) & Transmissivity (T_{TM}-dashed curve) spectra for TM waves at various angles of incidence. ($n_1 = 2.2$, $n_2 = 1.0$, $n_0 = n_s = 1.0$, $d_1 = 46\,\mathrm{nm}$, $d_2 = 192\,\mathrm{nm}$, $N = 10$).

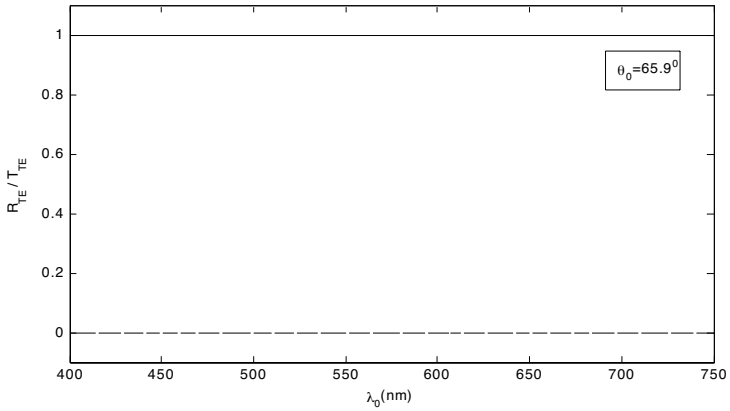

Figure 4.1. Reflectivity (R_{TE}-solid curve) & Transmissivity (T_{TE}-dashed curve) spectra for TE wave at Brewster's angle. ($n_1 = 3.4$, $n_2 = 1.52$, $n_0 = n_s = 1.52$, $d_1 = 46\,\mathrm{nm}$, $d_2 = 192\,\mathrm{nm}$, $N = 10$).

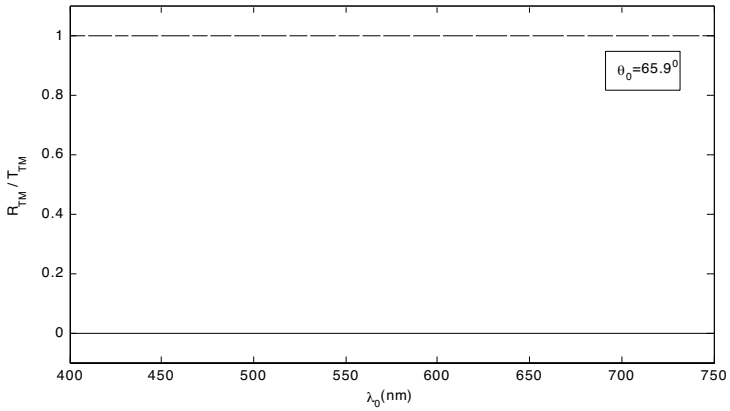

Figure 4.2. Reflectivity (R_{TM}-solid curve) & Transmissivity (T_{TM}-dashed curve) spectra for TM wave at Brewster's angle. ($n_1 = 3.4$, $n_2 = 1.52$, $n_0 = n_s = 1.52$, $d_1 = 46\,\mathrm{nm}$, $d_2 = 192\,\mathrm{nm}$, $N = 10$).

considered, whereas the TE wave [Fig. 2.1(d)] shows non zero reflectivity for a significant portion in this range, i.e., $R_{\mathrm{TM}} = 0$ and $R_{\mathrm{TE}} \neq 0$ simultaneously, indicating that the device is working as a polarizer by reflection. Also in the wavelength range 400 nm–428 nm, $R_{\mathrm{TE}} = 1$ (Table 1.2). Hence in this range the polarizer is most efficient in its operation giving enhanced intensity of polarized light. Comparison of curves 3.1(d) and 3.2(d) shows that the structure acts as a polarizer for an incidence angle of 65.20. Here $R_{\mathrm{TE}} = 1$

Table 1.1. Photonic band gaps at different angles of incidence.

Type of Structure	Angle of Incidence (θ^0)	PBG For TE Wave		PBG For TM Wave	
		Wavelength Range For $R_{TE} \approx 1$	PBG Width (nm)	Wavelength Range For $R_{TM} \approx 1$	PBG Width (nm)
$n_1 = 1.52, n_2 = 1.0$, $n_0 = n_s = 1.0$, $d_1 = 46$nm, $d_2 = 192$nm, $N = 10$.	0.0	508 - 544	36	508 - 544	36
	30.0	427 - 516	89	-	-
	45.0	400 - 472	72	-	-
	56.7	400 - 430	30	0	0
	75.0	-	-	-	-
	85.0	-	-	-	-
$n_1 = 2.2, n_2 = 1.0$, $n_0 = n_s = 1.0$, $d_1 = 46$nm, $d_2 = 192$nm, $N = 10$.	0.0	489 - 750	261	489 - 750	261
	30.0	426 - 719	293	449- 653	204
	45.0	400 - 683	283	409 - 534	125
	65.2	400 - 634	234	0	0
	75.0	400 - 618	218	-	-
	85.0	400 - 609	209	-	-
		614 - 631	17	-	-
		650 - 668	18	-	-

for a much wider range (400 nm–632 nm) as the photonic bandgap region has become wider due to a sharper refractive index contrast. The above investigations have been repeated with a different ambient medium ($n_0 = n_s = 1.52$). Taking $n_1 = 3.4$ (GaP), $n_2 = 1.52$ (glass), $d_1 = 46$ nm, $d_2 = 192$ nm, $N = 10$, the range of maximum reflectivity ($R_{\mathrm{TE}} = 1$) is achieved for the entire range (400 nm–750 nm) considered at Brewster's angle 65.90 (Fig. 4.1 & Fig. 4.2). Thus the desired wavelength range of maximum efficiency of operation of the polarizer can be achieved by changing the lattice parameters, or the refractive index of the ambient medium, or both.

It has been earlier reported [36] that for light incident on a glass slab ($n = 1.52$) from air, $R_{\mathrm{TM}} = 0$ and$R_{\mathrm{TE}} = 0.15$ at Brewster's angle 56.70. For air ($n = 1.0$), ZrO_2 ($n = 2.2$) interface $R_{\mathrm{TM}} = 0$ and $R_{\mathrm{TE}} = 0.42$ at Brewster's angle 65.20 (Fig. 5.1). For reflection from glass ($n = 1.52$) to GaP ($n = 3.4$) at Brewster's angle 65.90, $R_{\mathrm{TM}} = 0$

Table 1.1. Maximum efficiency range of polarizer for different PBG structure.

S.No.	Type of Structure	Brewster Angle$(\theta_B)^0$	Wavelength Range For $R_{TE}=1$	Wavelength Range For $R_{TM}=0$	Maximum Efficiency Range Of Polarizer(nm)
1.	$n_1 = 1.52, n_2 = 1.0$, $n_0 = n_s = 1.0$, $d_1 = 46\text{nm}, d_2 = 192\text{nm}$, $N = 10$.	56.7	400 - 428	400 - 750	400 - 428
2.	$n_1 = 2.2, n_2 = 1.0$, $n_0 = n_s = 1.0$, $d_1 = 46\text{nm}, d_2 = 192\text{nm}$, $N = 10$.	65.2	400 - 632	400 - 750	400 - 632
3.	$n_1 = 3.4, n_2 = 1.52$, $n_0 = n_s = 1.52$, $d_1 = 46\text{nm}, d_2 = 192\text{nm}$, $N = 10$.	65.9	400 - 750	400 - 750	400 - 750

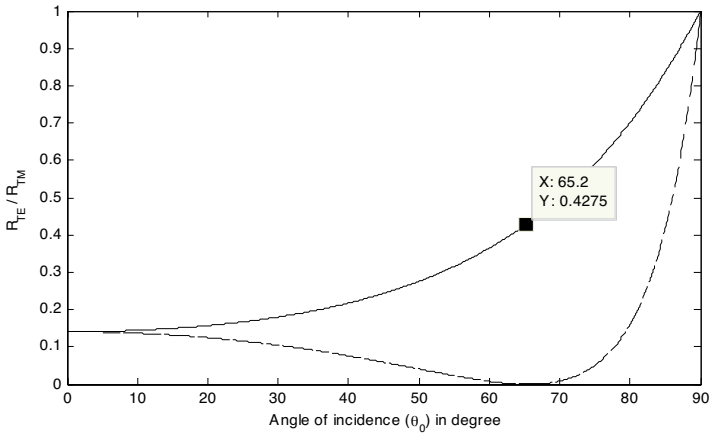

Figure 5.1. Reflectivity (R_{TE}-solid curve & R_{TM}-dashed curve) as a function of the angle of incidence for Air-ZrO_2 interface.

and $R_{\text{TE}} = 0.44$ (Fig. 5.2). Table 1.3 shows these results. Hence we conclude that a polarizer made by reflection from a PBG material is more efficient (giving a reflectivity of 100% in specific wavelength

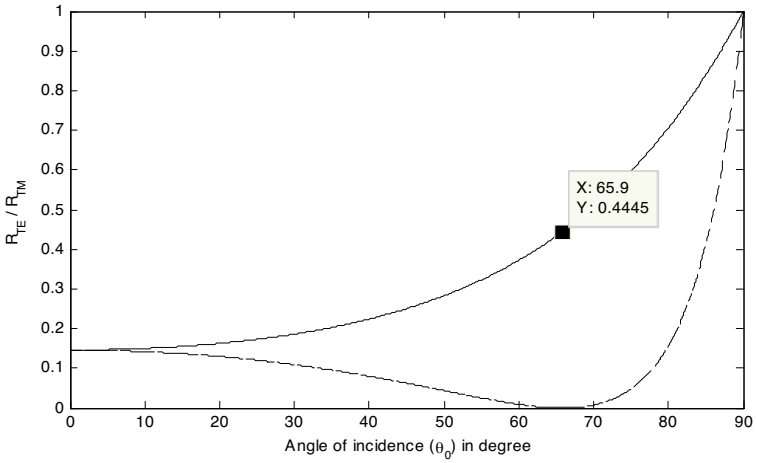

Figure 5.2. Reflectivity (R_{TE}-solid curve & R_{TM}-dashed curve) as a function of the angle of incidence for Glass-Gap interface.

Table 1.1. Reflectivity (R_{TE}, R_{TM}) at brewster angle (θ_B) [For single dielectric slab].

S.No.	Interface	Brewster Angle $(\theta_B)^0$	Reflectivity R_{TE}	Reflectivity R_{TM}
1.	Air - Glass(BK7)	56.7	0.15	0
2.	Air - ZrO_2	65.2	0.42	0
3.	Glass - GaP	65.9	0.44	0

ranges) as compared to that obtained by reflection from a single dielectric slab (which gives a comparatively much weaker intensity of polarized light).

5. CONCLUSION

In summary we have investigated the photonic bandgaps for glass ($n_1 = 1.52$)-air, ZrO_2 ($n_1 = 2.2$)-air, and GaP ($n_1 = 3.4$)-glass PBG structures and found that with increasing angle of incidence, the band gaps shift towards the lower wavelength side. Also with a sharper refractive index contrast, bandgap regions becomes wider. We have also suggested a polarizer with these structures which gives a much enhanced intensity of polarized light as compared to a polarizer obtained by reflection from a single dielectric slab.

ACKNOWLEDGMENT

One of the author Dr. Suneet Kumar Awasthi wishes to thank Dr. Ashok Kumar Chauhan, Founder President, Amity University, India for his constant interest and encouragement. The authors are thankful to Dr. T. P. Pandya and Dr. L. M. Bali for helpful discussions and for encouragement.

REFERENCES

1. Sigalas, M. M., C. M. Soukoulis, C. T. Chan, R. Biswas, and K. M. Ho, "Effect of disorder on photonic bandgaps," *Phys. Rev. B*, Vol. 59, 12767–12770, 1999.
2. Johnson, S. G. and J. D. Joannopoulos, "Introduction to photonic crystal: Bloch's theorem, band diagrams and gaps (but no defects)," *Photonic Crystal Tutorial*, 1–16, 2003, http://ab-initio.mit.edu/photons/tutorial/.
3. Yeh, P., A. Yariv, and C. S. Hong, "Electromagnetic propagation in periodic stratified media. I. General theory," *J. Opt. Soc. Am.*, Vol. 67, 423–438, 1977.
4. Sakoda, K., *Optical Properties of Photonic Crystals*, Springer, Germany, 2001.
5. Yablonovitch, E., "Inhibited spontaneous emission in solid state physics and electromagnetics," *Phys. Rev. Lett.*, Vol. 58, 2059, 1987.
6. Mekis, A., M. Meier, A. Dodabalapur, R. E. Slusher, and J. D. Joannopulos, "Lasing mechanism in two-dimensional photonic crystal lasers," *Appl. Phy. A: Materials Science and Processing*, Vol. 69, 111–114, 1999.
7. Painter, O., R. K. Lee, A. Scherer, A. Yariv, J. D. O'Brien, P. D. Dappus, and I. Kim, "Two-dimensional photonic band-gap defect mode laser," *Science*, Vol. 284, 1819–1821, 1999.
8. Noda, S., M. Yokoyama, M. Imada, A. Chutinan, and M. Mochizuki, "Polarisation mode control of two-dimensional photonic crystal laser by unit cell structure design," *Science*, Vol. 293, 1123–1125, 2001.
9. Knight, J. C., J. Broeng, T. A. Bieks, and P. S. J. Russell, "Photonic band gap guidance in optical fibers," *Science*, Vol. 282, 1476–1479, 1998.
10. Ziolkowski, R. W. and M. Tanaka, "FDTD analysis of PBG waveguides, power splitters and switches," *Opt. Quant. Electron*, Vol. 31, 843–855, 1999.

11. Ozbay, E., M. Bayindir, I. Bulu, and E. Cubukcu, "Investigation of localized coupled cavity modes in two-dimensional photonic bandgap structures," *IEEE Journal of Quantum Electronics*, Vol. 38, 837–843, 2002.
12. Zheng, Q. R., Y. Q. Fu, and N. C. Yuan, "Characteristics of planar PBG structures with a cover layer," *Journal of Electromagnetic Waves and Applications*, Vol. 20, 1439–1453, 2006.
13. Rojas, J. A. M., J. Alpuente, J. Piñeiro, and R. Sánchez, "Rigorous full vectorial analysis of electromagnetic wave propagation in 1D," *Progress In Electromagnetics Research*, PIER 63, 89–105, 2006.
14. Ozbay, E., B. Temelkuran, and M. Bayinder, "Microwave application of photonic crystals," *Progress In Electromagnetics Research*, PIER 41, 185–209, 2003.
15. Srivastava, R., S. Pati, and S. P. Ojha, "Enhancement of omnidirectional reflection in photonic crystal heterostructures," *Progress In Electromagnetics Research B*, Vol. 1, 197–208, 2008.
16. Zandi, O., Z. Atlasbaf, and K. Forooraghi, "Flat multilayer dielectric reflector antennas," *Progress In Electromagnetics Research*, PIER 72, 1–19, 2007.
17. Zhao, L. P., X. Zhai, B. Wu, T. Su, W. Xue, and C.-H. Liang, "Novel design of dual-mode bandpass filter using rectangle structure," *Progress In Electromagnetics Research B*, Vol. 3, 131–141, 2008.
18. Singh, S. K., J. P. Pandey, K. B. Thapa, and S. P. Ojha, "Structural parameters in the formation of omnidirectional high reflectors," *Progress In Electromagnetics Research*, PIER 70, 53–78, 2007.
19. Pandey, P. C., A. Mishra, and S. P. Ojha, "Modal dispersion characteristics of a single mode dielectric optical waveguide with a guiding region cross-section bounded by two involuted spirals," *Progress In Electromagnetics Research*, PIER 73, 1–13, 2007.
20. Osipov, A. V., I. T. Iakubov, A. N. Lagarkov, S. A. Maklakov, D. A. Petrov, K. N. Rozanov, and I. A. Ryzhikov, "Multi-layered Fe films for microwave applications," *PIERS Online*, Vol. 3, 1303–1306, 2007.
21. Shi, S. and D. W. Prather, "Lasing dynamics of a novel silicon photonic crystal cavity," *PIERS Online*, Vol. 3, 746–750, 2007.
22. Yatsyk, V., "Effects of the resonant scattering of intensive fields by weakly nonlinear dielectric layer," *PIERS Online*, Vol. 3, 524–527, 2006.

23. Brongersma, M. L., R. Zia, and J. Schuler, "Plasmonics — The missing link between nanoelectronics and microphotonics," *PIERS Online*, Vol. 3, 360–362, 2007.
24. Hou, S. and C. Hu, "Influence of electro-optic effecton waveguide efficiency of optical fiber with cladding made of uniaxial crystal materials," *PIERS Online*, Vol. 2, 614–618, 2006.
25. Li, L., C.-H. Liang, and C. H. Chan, "Waveguide end slot phased array antenna integrated with electromagnetic bandgap structures," *J. Electromagnetic Waves and Applications*, Vol. 21, 161–174, 2007.
26. Kokkorakis, G. C., "Calculating the electric field in nanostructures," *J. Electromagnetic Waves and Applications*, Vol. 21, 1433–144, 2007.
27. Li, L. and J. A. Dobrowolski, "Visible broadband, wide-angle, thin-film multilayer polarizing beam splitter," *Appl. Opt.*, Vol. 35, 2221–2225, 1996.
28. Hecht, E., *Optics*, 4th edition, 349, Addison Wesley, 2002.
29. Yeh, P., "Optics of periodic layered media," *Optical Waves in Layered Media*, 118–142, Wiley, New York, 1998.
30. Born, M. and E. Wolf, "Basic properties of the electromagnetic field," *Principles of Optics*, 1–70, Cambridge University Press, U.K., 1980.
31. Dowling, J. P. and C. M. Bowden, "Anomalous index of refraction in photonic band gap materials," *J. Mod. Optics*, Vol. 41, 345–351, 1994.
32. John, S. and J. Wang, "Quantum optics of localized light in a photonic band gap," *Phys. Rev. B*, Vol. 43, 12772–12789, 1991.
33. Liu, N.-H., "Propagation of light waves in Thue-Morse dielectric multilayers," *Phys. Rev. B*, Vol. 55, 3543–3547, 1997.
34. Liu, N.-H., "Defect modes of stratified dielectric media," *Phys. Rev. B*, Vol. 55, 4097–4100, 1997.
35. Born, M. and E. Wolf, "Basic properties of the electromagnetic field," *Principles of Optics*, 60, Cambridge University Press, U.K., 1980.
36. Born, M. and E. Wolf, "Basic properties of the electromagnetic field," *Principles of Optics*, 44, Cambridge University Press, U.K., 1980.